*35th EPS Conference on Plasma Phys. Hersonissos, 9 - 13 June 2008 ECA Vol.**32D**, P-2.080 (2008)*

RWM control in ITER including a realistic 3D geometry

F. Villone[1], R. Albanese[2], G. Ambrosino[2], Y. Q. Liu[3], A. Pironti[2], A. Portone[4], G. Rubinacci[2]

[1]*Ass. Euratom/ENEA/CREATE, Università di Cassino, Italy*

[2] *Ass. Euratom/ENEA/CREATE, Università Federico II di Napoli, Italy*

[3] *EURATOM/UKAEA Fusion Association, Culham Science Centre, Abingdon, UK*

[4] *Fusion for Energy, Barcelona, Spain*

Plasma perturbations due to ideal, pressure driven external kink unstable modes induce, in a conducting nearby wall, eddy currents which may have a stabilizing effect. Due to eddy currents decay, related to the non-zero resistivity of the surrounding wall, the resulting resistive wall modes (RWM) grow on a time scale of the order of the wall time.

In ITER, non-axisymmetric coils can be used to actively stabilize such modes. To evaluate the performances of a controller it is fundamental to accurately model the plasma response to such coils, including the effects of 3D active and passive conducting structures.

To this purpose, we apply to ITER the recently developed CarMa code [1-3], that allows a rigorous and self-consistent treatment of any three dimensional conducting structure. The mathematical model obtained has the same form as for the axisymmetric vertical instability [4]; hence, all the existing tools of system theory can be used. In particular, it is possible to calculate the so-called Best Achievable Performances, quantifying the maximum performance that any control system can achieve with given voltage limitations on control coils.

The CarMa computational tool [3]

The main assumption made is to neglect plasma mass, which is a good approximation since in ITER the RWM growth time is typically much slower than the Alfvén time.

A surface S is chosen, in between the plasma and the conducting structures. The plasma (instantaneous) response to a given magnetic flux density perturbation on S is computed as a plasma response matrix, using the MARS-F code [5]. With such plasma response matrix, the effect of 3D structures on plasma is evaluated by computing the magnetic flux density on S due to 3D currents. The currents induced in the 3D structures by plasma are described using a volumetric time-domain integral formulation of the eddy currents equations [6], which requires a finite elements discretization of the conducting structures only. The induced currents are computed via an equivalent surface current distribution on S providing the same magnetic field as plasma outside *S*. The overall plasma response model can be recast in state-space form [3]:

$$\frac{d\underline{I}}{dt} = \underline{\underline{A}}\,\underline{I} + \underline{\underline{B}}\,\underline{V}, \quad \underline{y} = \underline{\underline{C}}\,\underline{I} \tag{1}$$

where $\underline{I}$ is the vector of discrete currents in the 3D structure (state vector), $\underline{V}$ is the vector of control coil voltages (input vector), $\underline{y}$ is the vector of magnetic field perturbations at given measurement points and $\underline{\underline{A}}$, $\underline{\underline{B}}$, $\underline{\underline{C}}$ are the dynamical, input and output matrices respectively.

The Best Achievable Performances

Considering n=1 unstable RWMs, the matrix $\underline{\underline{A}}$ in equation (1) has a pair of unstable eigenvalues $\alpha \pm j\omega$ $(\alpha > 0, \omega \geq 0)$, corresponding to unstable eigenmodes that are shifted of $\pi/2$ in the toroidal direction [3]. These modes have to be stabilized by using the available control coils, which are voltage driven by suitable power supplies. The voltage and currents limits of the power supplies constraint the amplitude of the maximum perturbations which can be recovered. A method to evaluate such maximum perturbations is the evaluation of the null controllable region of system (1) [7] when the power supplies are subject to a given maximum voltage constraints. Hence, we assume that each component V_i of vector $\underline{V}$ is admissible when it satisfies the inequalities $-V_{Mi} \leq V_i \leq V_{Mi}$, where V_{Mi} is the maximum voltage available on the i-th power supply.

An initial 3D current distribution $\underline{I}_0$ *is said to be null controllable, if there exists a finite time* t_f *and an admissible control voltage law* $\underline{V}(t)$ *such that the state trajectory* $\underline{I}(t)$ *of the system (1) satisfies* $\underline{I}(0)=\underline{I}_0$, $\underline{I}(t_f)=0$. *The set of all null controllable states is called the null controllable region of the system (1).*

By a suitable state space transformation $\underline{x}=\underline{\underline{T}}\,\underline{I}$, system (1) can be rewritten as follows:

$$\frac{d}{dt}\begin{bmatrix} x_1 \\ x_2 \\ \underline{x}_s \end{bmatrix} = \begin{bmatrix} \begin{bmatrix} \alpha & -\omega \\ \omega & \alpha \end{bmatrix} & \underline{\underline{0}} \\ \underline{\underline{0}} & \underline{\underline{A}}_s \end{bmatrix} \begin{bmatrix} x_1 \\ x_2 \\ \underline{x}_s \end{bmatrix} + \begin{bmatrix} \underline{\underline{B}}_u \\ \underline{\underline{B}}_s \end{bmatrix} \underline{V} \tag{2}$$

The $n_s \times n_s$ matrix $\underline{\underline{A}}_s$ contains the stable modes of system (1). The null controllable region of systems (1) and (2) are isomorphic under the transformation $\underline{\underline{T}}$, so it possible to work directly with representation (2). A procedure to evaluate this null controllable region, outlined in [7], is based on solving a suitable optimal control problem for the reduced order system:

$$\frac{d}{dt}\begin{bmatrix} x_1 \\ x_2 \end{bmatrix} = \begin{bmatrix} \alpha & -\omega \\ \omega & \alpha \end{bmatrix} \begin{bmatrix} x_1 \\ x_2 \end{bmatrix} + \underline{\underline{B}}_u \underline{V}, \tag{3}$$

which contains only the two unstable modes. Once the null controllable region has been evaluated, using the output mapping in equation (1), it is possible to characterize the maximum allowable perturbations as initial (i.e. at t=0) displacements of the magnetic fields measured by the sensors. These maximum initial displacements define the so-called best achievable performances.

Results

The ITER geometry has been represented with a high level of details (Fig. 1): double shell, outer triangular support, port extensions, active coils.

First of all, we have made an open-loop analysis of growth rates for various values of β_N. Table 1 reports the results for the mesh of Fig. 1 (with port extensions) and for a simplified mesh with the ports represented simply by patches with a varying resistivity η_H. The results suggest that purely 2D estimates (i.e. with patches having the same resistivity as vessel) can underestimate the results (about 20-40% for moderate growth rates), while replacing the ports with pure holes ($\eta_H \rightarrow +\infty$) can be severely pessimistic (more than 50%). With a value $\eta_H = 4\cdot 10^{-6}\ \Omega\mathrm{m}$, it is possible to reasonably estimate the growth rate in the whole β_N range.

We have considered the ITER external coils, intended for error field correction, as possible actuators for RWM control. Figure 2 reports a typical result of the analysis of the best achievable performances for the equilibrium with the lowest β_N, in which y_1 and y_2 are:

$$y_1(t) = \frac{2}{N}\sum_{k=1}^{N} B_k(t)\cos(\phi_k) \qquad\qquad y_2(t) = \frac{2}{N}\sum_{k=1}^{N} B_k(t)\sin(\phi_k) \qquad (4)$$

and $B_k(t)$ are $N=18$ measurements of the vertical magnetic field in the outboard region at equally spaced toroidal angles φ_k. The perturbations corresponding to points in the interior of the polygons can be stabilized with the given voltage saturation level. The hexagonal shape of the boundary is due to the fact that there are six external coils (fed in antiseries by three actuators). This work was supported in part by Italian MiUR under PRIN grant 2006094025 and in part by Consorzio CREATE.

β_N	Port extensions	2D estimate	$\eta_H = 4\cdot 10^{-6}\ \Omega\mathrm{m}$	Holes
2.86	7.64	5.99	8.25	11.3
3.02	15.4	11.5	16.1	24.3
3.17	30.0	20.9	29.6	51.8
3.33	69.0	41.5	59.9	155
3.48	272.0	98.9	148.1	N.A.

Table 1. Growth rates (in s^{-1}) for various values of normalized β_N.

References

[1] F. Villone et al., *34th EPS Conference*, Warsaw, July 2007, paper P5.125

[2] R. Albanese et al., *IEEE Trans. Mag.* **44** (2008) pp. 1654-1657

[3] A. Portone, F. Villone, et al., *Plasma Phys. Contr. Fus.* **50** (2008) 085004

[4] R. Albanese, F. Villone, *Nuclear Fusion*, vol. 38, no. 5, pp. 723-738, May 1998.

[5] Y. Q. Liu and A. Bondeson, *Phys. Rev. Lett.* **84** (2000) 907

[6] R. Albanese, G. Rubinacci, *IEE Proc.* Part A **135** (1988) 457–462

[7] T. Hu, Z. Lin, *International Journal of Robust and Nonlinear Control*, **11**(2001) 555

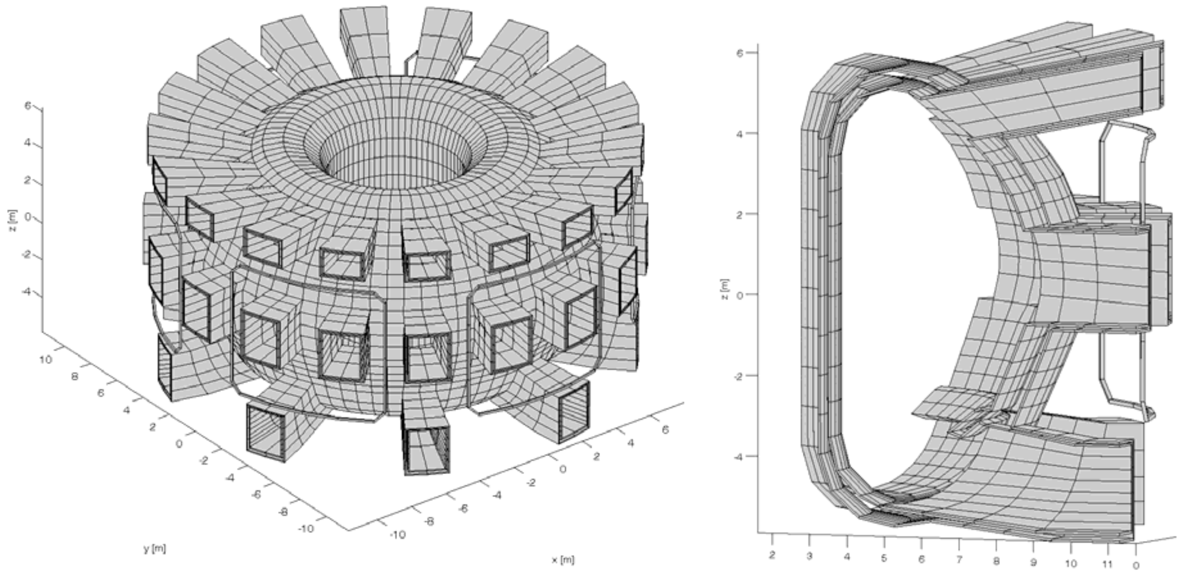

Fig. 1. Discretization of ITER geometry: overall view and cutaway figure.

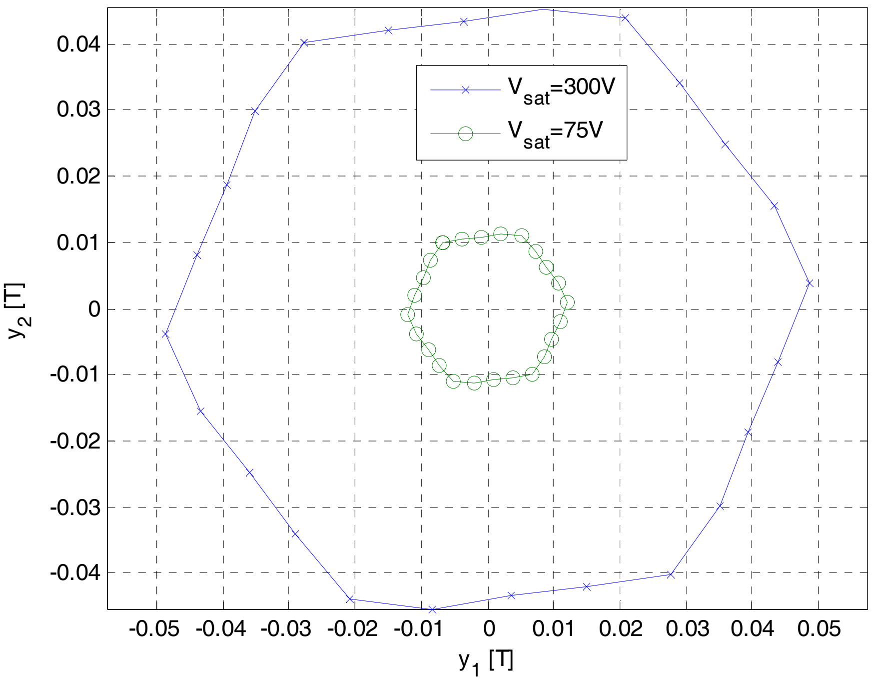

Fig. 2. Best Achievable Performances.